ALKU Journal of Science 2023, Sayı 5 (3): 163-175
e-ISSN: 2667-7814

Original Article

Optimization Studies of Mg/Al-NO_3 Layered Double Hydroxide Nanoparticles by Hydrothermal Treatment

Kevser Bal[1*], Sema Şentürk[1], Özlem Kaplan[2], Mehmet Koray Gök[1], Saadet Kevser Pabuccuoğlu[1]

[1]*Istanbul University-Cerrahpasa, Faculty of Engineering, Department of Chemical Engineering, Istanbul, Turkey*

[2]*Alanya Alaaddin Keykubat University, Rafet Kayış Faculty of Engineering, Department of Genetics and Bioengineering, Antalya, Turkey*

**kevser.bal@iuc.edu.tr*

Abstract

Layered Double Hydroxide-based nanoparticles offer significant advantages in biological applications with high biocompatibility and low cytotoxicity. In this study, nanoparticles (nMg/Al-NO_3-LDH) were synthesized by the co-precipitation method, and synthesis optimization of the nanoparticles was carried out by hydrothermal treatment. The effect of hydrothermal treatment on Z-average and surface charge was evaluated. Experiments were performed at 80˚C and 100˚C in the range of 2-48 h by using different stirring rates (250, 1000, and 1500 rpm) and without stirring. Dynamic Light Scattering (DLS) was used to assess the particle size (nm), polydispersity index (PDI), and zeta potential (mV) of the nanoparticles. The chemical structure of nanoparticles was characterized by Fourier Transform Infrared spectrometry (FTIR). As a result, nanoparticles with an optimum particle size of 86.87 nm, a PDI of 0.132, and a zeta potential (mV) of 44.4±8.74 were obtained at 80˚C, 48h and 250 rpm. The data showed that Mg/Al-NO_3-LDH nanoparticles have suitable physical properties for biological applications.

Keywords: Layered double hydroxide nanoparticles, Hydrothermal treatment, Particle size optimization, Inorganic materials

Mg/Al-NO_3 Çift Tabakalı Hidroksit Nanopartiküllerinin Hidrotermal İşlem İle Optimizasyonu Çalışmaları

Özet

Çift Tabakalı Hidroksitler yüksek biyouyumluluk ve düşük sitotoksisite ile biyolojik uygulamalarda önemli avantajlar sunar. Bu çalışmada nanopartiküller (nMg/Al-NO_3-LDH) birlikte çöktürme yöntemiyle sentezlendi ve nanopartiküllerin sentez optimizasyonu hidrotermal işlem altında gerçekleştirildi. Hidrotermal işlemin partikül boyutu ve yüzey yükü üzerindeki etkisi değerlendirildi. Deneyler 80˚C ve 100˚C'de, 2-48 saat aralığında ve çeşitli karıştırma hızlarında 250, 1000, 1500 rpm gerçekleştirildi. Nanopartiküllerin partikül boyutu (nm), polidispersite indeksi (PDI) ve zeta potansiyel (mV) değerleri Dinamik Işık Saçılımı (DLS) ile saptandı. Nanopartiküllerin kimyasal yapısı Fourier Dönüşümü Kızılötesi spektrometresi (FTIR) ile karakterize edildi. Sonuç olarak, 80˚C, 48 saat ve 250 rpm'de optimum partikül boyutu 86.87 nm, polidispersite indeksi (PDI) 0.132 ve zeta potansiyeli (mV) 44.4±8.74 olan nanopartiküller elde edildi. Veriler, biyolojik uygulamalarda kullanıma yönelik Mg/Al-NO_3-LDH nanopartiküllerinin uygun fiziksel özelliklere sahip olduğunu gösterdi.

Anahtar Kelimeler: Çift tabakalı hidroksit nanopartiküller, Hidrotermal işlem, Partikül boyutu optimizasyonu, İnorganik malzemeler

Geliş/Received: 3 Ekim/October 2023
Kabul Ediliş/Accepted: 20 Ekim/October 2023

1. INTRODUCTION

Layered Double Hydroxides (LDHs) are layered materials with a unique 2-dimensional structure and biocompatibility. The alternating pattern of positively charged metal hydroxide layers and negatively charged interlayer exchangeable anions characterizes them [1]. LDHs have recently gained popularity due to their unique properties and versatile applications in various fields, including catalysis, drug delivery, and environmental remediation [2]. LDH has superior properties such as good biocompatibility, low cytotoxicity, high loading capacity, diverse functionality, tunable particle size, targeted delivery, and protection of biomolecules from external chemical and biological attacks [3]. Numerous research has focused on the utilization of LDH as a carrier of biomolecules such as vitamins [4], anti-inflammatory drugs [5], anti-cancer drugs [6], neurodegenerative drugs [7] and genes [8,9]. In synthesizing LDH nanoparticles, the co-precipitation method is a widely used technique known for its simplicity and efficiency in producing well-defined nanostructures [10].

LDH possesses a general chemical formula of $[M^{II}_{1-x} M^{III}_{x}(OH)_2]^{x+} (A^{n-})_{x/n} \cdot mH_2O$, wherein M^{II}, M^{III} and A^{n-} represent divalent a metal cation, a trivalent metal cation and an interlayer anion, respectively. LDH has a layered crystal structure that varies widely depending on the structure of the cations M^{II}/M^{III} molar ratios and anion type. The range $0.2 < x < 0.33$ (M^{II}/M^{III} ratio between 2: 1 and 4: 1) is suitable for pure LDH synthesis. In the case of $x > 0.33$, the formation of $M(OH)_3$ occurs; likewise, $M(OH)_2$ is formed at $x < 0.2$ [11,12].

Hydrothermal treatment is an important step in improving the properties of LDH nanoparticles, as it allows fine-tuning parameters such as temperature, time, and stirring speed [13]. In this study, the synthesis of nMg/Al-NO_3-LDH was optimized for use in biological applications. nMg/Al-NO_3-LDH was prepared by the co-precipitation method, and the hydrothermal optimization of the nMg/Al-NO_3-LDH was examined. It is well established in biological applications that parameters such as cellular uptake, biodistribution, and biocompatibility are significantly influenced by particle size and surface charge [14].

In this regard, the effect of synthesis conditions such as temperature, time, and stirring rate on the particle characteristics was investigated. The size (nm), PDI and zeta potential (mV) of nMg/Al-NO_3-LDH prepared under various conditions were revealed by Dynamic Light Scattering (DLS) analysis, while their chemical structure was illuminated by Fourier Transform Infrared Spectrometer (FT-IR). Especially there is no study on the nanoparticle size of stirring rate during hydrothermal treatment, but the data obtained with this parameter created a meaningful and important result and brought innovation and originality to our study.

2. MATERIAL AND METHOD

2.1 Material

Mg $(NO_3)_2.6H_2O$ (>99%) and Al $(NO_3).9H_2O$ was obtained from Merck. NaOH (>98-100) purchased from Sigma–Aldrich.

2.2 Synthesis and Optimization of nMg/Al-NO_3-LDH

nMg/Al-NO_3-LDH were synthesized using a coprecipitation step followed by a hydrothermal treatment process [15]. 10 mL aqueous solution of 3 mmole Mg $(NO_3)_2.6H_2O$, and 1 mmole Al $(NO_3).9H_2O$, ([Al]/([Mg]+[Al]); 0.25) was added quickly in NaOH solution (0.15 M, 40 mL) under vigorous magnetic stirring continued for 10 min. This acquired LDH suspension was separated by centrifuging for 5 min at 4500 rpm. LDH slurry was washed, dispersed in 50 mL of deionized water, and transferred into an autoclave (Berghof Highpreactor BR-HS; Germany). Hydrothermal treatments were carried out at 80˚C and 100˚C, in a range of 2-48 h and with different stirring rates (250, 1000, and 1500 rpm) and without stirring, respectively. Figure 1 depicts the synthesis of Mg/Al-NO3-LDH nanoparticles.

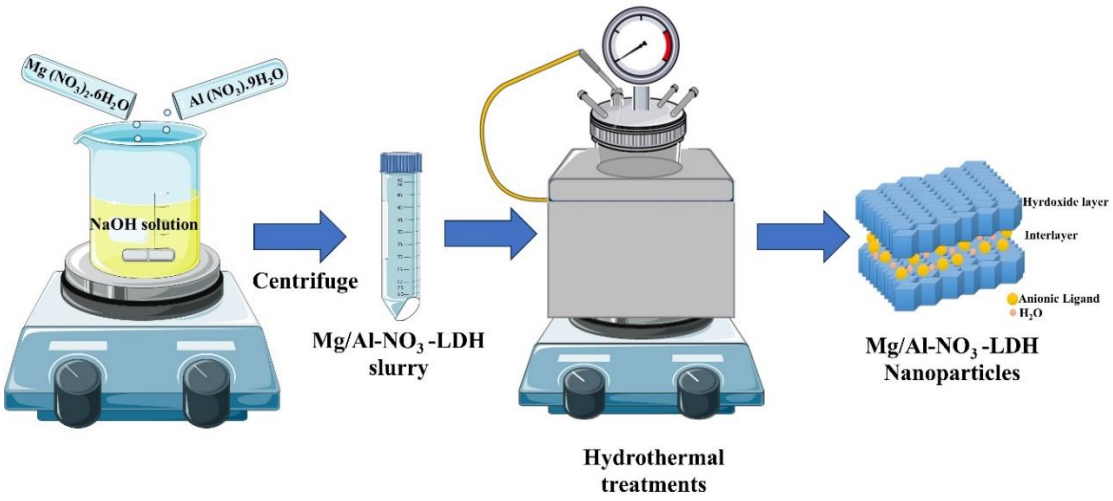

Figure 1. Schematic illustration of nMg/Al-NO_3-LDH synthesis

After the co-precipitation process, the effect of hydrothermal treatment conditions was examined by changing the temperature, stirring rate and time on nanoparticle characteristics. First, the hydrothermal treatment process was examined for the different stirring rates (250 rpm, 1000 rpm, 1500 rpm). For this purpose, samples were taken at different time intervals for different stirring rates, and then particle size (nm), PDI, and zeta potential (mV) values were determined. Secondly, the effect of temperature (80°C and 100°C) was examined after determining the appropriate stirring rate. Finally, the effect of hydrothermal treatment time (2h, 4h, 6h, 8h, 24h and 48 h) on particle size, PDI, and zeta potential value was also examined.

2.3. Characterization of nMg/Al-NO_3-LDH

2.3.1 FTIR analysis

The structure of nMg/Al-NO_3-LDH was identified on a Fourier transform infrared (FTIR) (Agilent Cary 630, USA) using a pellet prepared with 1 mg of the sample and 200mg of KBr. The absorption spectra were obtained in the wavenumber range of 4000-650 cm^{-1}.

2.3.2 Determination of mean particle size, PDI and zeta potential

Photon correlation spectroscopy (Nano ZS, Malvern UK) was used to determine the Z-average and PDI of nMg/Al-NO_3-LDH. The same instrument was used to determine the surface charge of nanoparticles. The measurement results were repeated three times.

2.4 Colloidal Stability of nMg/Al-NO_3-LDH

The colloidal stability of nMg/Al-NO_3-LDH was examined by storing dispersions at +4 ± 1 °C. Particle size, PDI, and zeta potential value were measured by taking weekly samples. Stability was checked over 5 weeks, and the measurement results were repeated three times.

2.5 Statistical Evaluation

Statistical analysis and similar data sets were analyzed using GraphPad Prism 8.0 software and a two-way ANOVA with the Sidak test. Statistical significance was evaluated as a probability value of 0.05.

3. RESULTS AND DISCUSSION

3.1 Synthesis and Characterization of nMg/Al-NO_3-LDH

As aforementioned in section 2.2, nMg/Al-NO_3-LDH was synthesized by the co-precipitation method using the magnesium and aluminum salts. Afterward, the stable suspension containing nMg/Al-NO_3-LDH was obtained by hydrothermal treatment. To elucidate the resulting structure, the nMg/Al-NO_3-LDH suspension was lyophilized, and the structure was characterized by FTIR analysis using the dry sample.

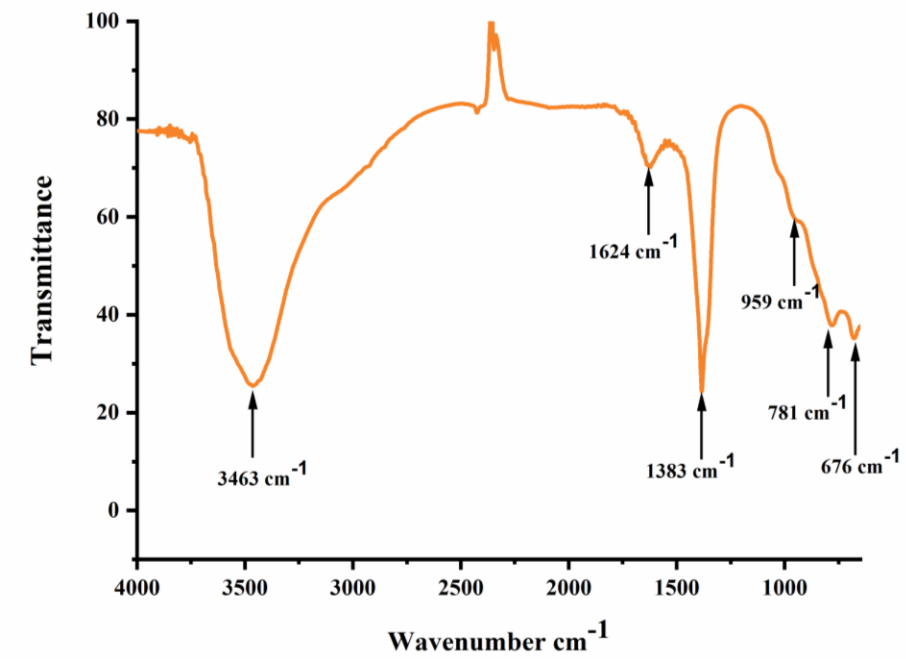

Figure 2. FTIR spectra of nMg/Al-NO_3-LDH

As illustrated in Figure 2, FTIR spectra of nMg/Al-NO_3-LDH are taken for the range of 4000-650 cm^{-1}. The broad absorption band in the 3250-3800 cm^{-1} region (maximum appeared at about 3463 cm^{-1}) and the broad shoulder appeared at about 3580 cm^{-1} are related to the symmetrical and asymmetric vibrations of the hydrogen-bonded O-H groups in lattice structure (Mg/Al-OH or Al-OH) and interlayer water molecules surrounding the exchangeable anions [16]. The small sharp absorption band seen at 1624 cm^{-1} is attributed to the deformation and bending vibrations of the H_2O molecules in the H_2O-CO_3^{2-} structure. The sharper band at about 1383 cm^{-1} was also assigned to the stretching vibrations of the NO_3^- anions in the interlayer region. The broad shoulder at about 1359 cm^{-1} was also assigned to the symmetric stretching vibrations of the unidentate CO_3^{2-} anions, which may have entered the structure during precipitation or purification. Hence, CO_3^{-2} and NO_3^{-1} anions in the interlayer of LDH are observed to be overlapped as the one sharp absorption band at 1383 cm^{-1} [4]. Absorption bands are seen as small sharp or small shoulders of approximately 500-1000 cm^{-1} caused by vibrations of the LDH lattice structure, which are Mg-O / Al-O / O-Al-O / O-Mg-O, Al-OH, H_2O molecules [17]. Consequently, FTIR spectra of nMg/Al-NO_3-LDH confirm its molecular structure.

3.2 Optimization Studies of nMg/Al-NO_3-LDH

Nanoparticulate systems are a very important developing field as drug or gene carrier systems [18]. It is known that the key factor to achieve maximum therapeutic effectiveness in the applications of these systems is the control of particle size, PDI and surface charge [14]. Additionally, some studies have revealed that

the particle size and surface charge of nanoparticles are more important than the nanoparticle structure in biological applications [14].

In optimizing the synthesis of nMg/Al-NO_3-LDH, the effect of hydrothermal treatment conditions such as time (2h, 4h, 6h, 8h, 24h), stirring rate (250 rpm, 1000 rpm and 1500 rpm) and without stirring on the characteristics of the nanoparticles were investigated at the constant temperature 100°C, which indicated in the literature [19-24]. According to the results (Figure 3), hydrothermal treatment conditions significantly affect particle size and PDI. As known, hydrothermal treatment increases the kinetic energy and Brownian motion that can overcome the adhesive effect and interaction between aggregates [19]. Thus, stable LDH suspension is obtained due to electrostatic repulsion between positive particles. The obtained values in Figure 3 show that the Z-average size varies between 77.47±0.150 nm and 133.8±3.195 nm due to the stirring rate. Moreover, hydrothermal treatments were carried out with and without stirring in the autoclave to observe the effect on particle size. All nMg/Al-NO_3-LDH were obtained smaller than 200 nm particle size at hydrothermal treatment conditions with variable stirring rate and time in the autoclave. This range is considered small-sized for nanoparticular systems [25] and a suitable agent for drug/gene carrier systems in target therapies [26-28]. Especially when the stirring rate is 250 rpm, it can be seen that all the results are below 100 nm (Table 1). This situation creates a great advantage for nanoparticle systems that target the blood-brain barrier, especially requiring small nanoparticle size (<200 nm) [29].

The PDI is defined as the level of non-uniformity in the size distribution of particles [30]. If the PDI value of the nanoparticle system is <0.1, it is highly uniform, and if it is between 0.1 and 0.4, it is considered to be moderately uniform. These two ranges are considered suitable for nanoparticular systems for drug/gene delivery systems [27,28,31]. If this value is >0.4, it indicates a high level of nanoparticle size variation and is unsuitable for drug/gen carrier systems [32]. Based on this, when we examined the PDI values, it was observed that the measured values varied between 0.185±0.014 and 0.404±0.0122 (Figure 3). In fact, all the obtained results have a good PDI value, of course, considering that specific values will be required depending on the carrier system to be customized.

Zeta potential, also called electrokinetic potential, is measured by the movement of particles dispersed in a liquid towards the positive or negative domain depending on the surface charge ratio when an electrical field is applied to the liquid [32]. Zeta potential is a highly significant characteristic of colloids or nanosuspension, and its value is strongly connected to suspension stability and particle surface shape. It is evaluated as a parameter of the impacts of pH, ionic strength, and the kind of ions in suspension [33,34]. When we examined all the zeta potential results, the values (between 37.8±6.39 and 51.4±6.82) were close to each other (Figure 3). The distribution is considered stable in colloidal systems where the zeta potential is higher than +30 mV or lower than −30 mV [35]. Accordingly, the results show that LDH nanoparticles with high cationic charge are stable.

According to Figure 3, the diversity in stirring rate resulted in a statistically significant change in particle size and PDI values, while the change in zeta potential was statistically insignificant at all times tested. However, when the stirring rate increased to 1500 rpm, particle size, PDI, and zeta potential value also increased due to increasing the intraparticle interaction. The obtained results revealed that the optimal stirring rate is 250 rpm.

Based on the literature, there are many studies on LDH [19,34]. Although there are different studies on parameters such as anion type in the structure, temperature, concentration and time, no study has been found investigating the effects of stirring speed on particle size, PDI and zeta potential in hydrothermal treatment. When the data obtained is examined, it shows that stirring rate is a statistically significant parameter of particle size in hydrothermal treatment. The stirring rate in the hydrothermal treatment on LDH nanoparticle creates a unique value for this study and distinguishes it from other studies.

Table 1. The zeta potential, particle size and PDI values of nMg/Al-NO_3-LDH obtained hydrothermal treatment conditions (250rpm, 100˚C, 24h)

	Time (h)	***Z-average (nm) ±SD***	***PD ±SD***	***Zeta potential (mV) ±SD***
100 ˚C-0 rpm	2 h	108,0±1,761	0,185±0,014	43,6±5,46
	4 h	105,0±0,5	0,210±0,003	45,1±7,51
	6 h	102,4±0,585	0,280±0,020	48,1±9,31
	8 h	100,0±1,217	0,245±0,004	42,4±5,86
	24 h	106,9±0,556	0,231±0,009	37,8±6,39
100°C -250 rpm	2 h	79,97±0,527	0,250±0,001	40,1±8,58
	4 h	77,47±0,150	0,211± 0,004	43,9±7,92
	6 h	77,59±0,820	0,192±0,013	45,6±7,74
	8 h	85,0±0,686	0,211±0,007	45,1±7,15
	24 h	95,10±0,707	0,201±0,004	44,8±6,87
100 ˚C-1000 rpm	2 h	106,9±0,862	0,247±0,006	43,7±53,8
	4 h	81,82±0,841	0,254±0,010	43,3±14,7
	6 h	77,18±0,31	0,229±0,004	44,2±6,37
	8 h	81,07±0,520	0,237±0,008	42,9±5,49
	24 h	86,34±0,89	0,208±0,011	42,7±8,62
100 ˚C-1500 rpm	2 h	93,68±0,826	0,404±0,0122	50,0±8,51
	4 h	99,02±2,933	0,378±0,006	51,2±8,42
	6 h	99,74±1,065	0,382±0,006	50,0±3,6
	8 h	104,0±2,592	0,380±0,005	51,4±6,82
	24 h	133,8±3,195	0,376±0,017	49,9±8,58

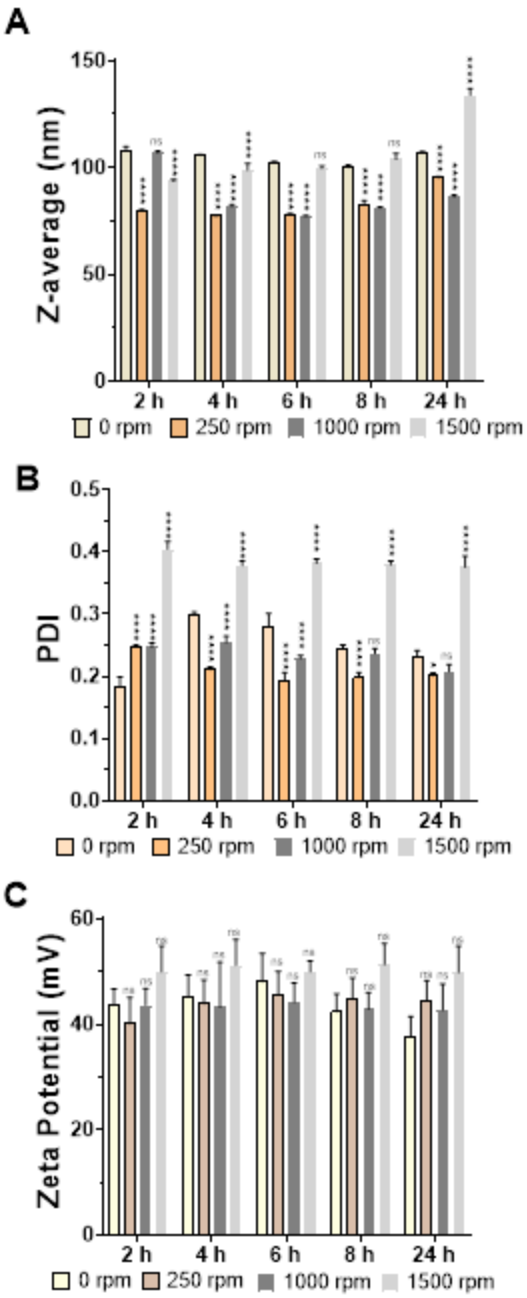

Figure 3. The particle size (nm) (A), PDI (B) and Zeta potential (mV) (C) of nMg/Al-NO_3-LDH in various parameters 0 (without stirring), 250, 1000 and 1500rpm. The data is provided as mean SEM (n = 3). The following statistical significance levels were used: *p < 0.05, **p < 0.01, ***p < 0.001, and ****p < 0.0001, ns: not significant.

To investigate the impact of temperature on the size and surface charge of nMg/Al-NO_3-LDH the stirring rate was kept constant at 250 rpm and the synthesis was carried out at 80°C. When the temperature was changed to 80°C, particle size and size distribution decreased at 24h, with no significant change in surface charge (Figure 4 and Table 2).

Table 2. Effect of temperature on the particle size (A), PDI (B) and zeta potential (C)

	Time (h)	*Z-average (nm) ±SD*	*PD ±SD*	*Zeta potential (mV) ±SD*
80°C – 250 rpm	2h	93,92±0,382	0,238±0,0122	44,6±6,52
	4 h	75,54±0,337	0,272±0,250	44,2±5,46
	6 h	73,86±0,864	0,208±0,0057	45,1±4,49
	8 h	77,72±1,130	0,224±0,005	45,3±3,95
	24 h	88,35±1,751	0,173±0,012	47,5±6,25

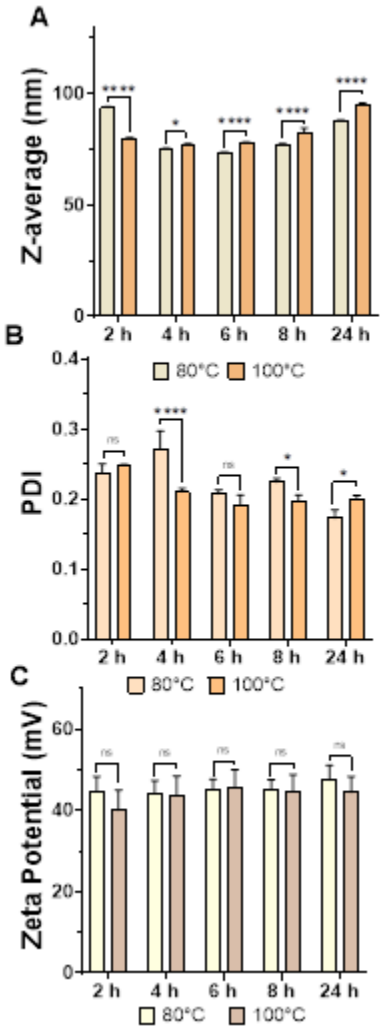

Figure 4. Effect of temperature on the particle size (A), PDI (B) and zeta potential (C)
The data is provided as mean SEM (n = 3). The following statistical significance levels were used: *p < 0.05, **p < 0.01, ***p < 0.001, and ****p < 0.0001, ns: not significant.

The particle size and PDI value of nMg/Al-NO_3-LDH are positively affected depending on hydrothermal treatment time (Table 3). Without hydrothermal treatment, LDH slurry has a glue effect causing aggregation, distribution over a wide range and a large PDI value.

Table 3. Effect of hydrothermal treatment time on the LDH particle size, PDI and zeta potential in 80˚C temperature, 250 rpm stirring rate.

Time (h)	*Z-average (nm)*	*PDI*	*Zeta potential (mV) ±SD*
without hydrothermal treatment	358.8±4,747	0.513±0,027	-
24	88.35±1,75	0.173±0,019	47.5±6.25
48	86.87±0.320	0.132±0,018	44.4±8.74

When the hydrothermal treatment time reached 24 h, it was seen that the nMg/Al-NO_3-LDH was a stable monodisperse nanosuspension with narrower size distributions i.e. lower PDI. However, a peak of about 1% is seen around 5000 nm of hydrothermal treatment time at 24 h. Therefore, the hydrothermal treatment time was raised to 48 h. Thus, it was observed that the unwanted second peak (~5000 nm) disappeared and the PDI value decreased significantly (Figure 5). According to the measurement results, the particle size was close to 24 h, but the PDI value was further decreased, and the large particles around 5000 nm turned into nanoparticular structure. In light of these findings, it was concluded that the most suitable hydrothermal treatment conditions were 80 °C, 250 rpm and 48 h to obtain the nMg/Al-NO_3-LDH.

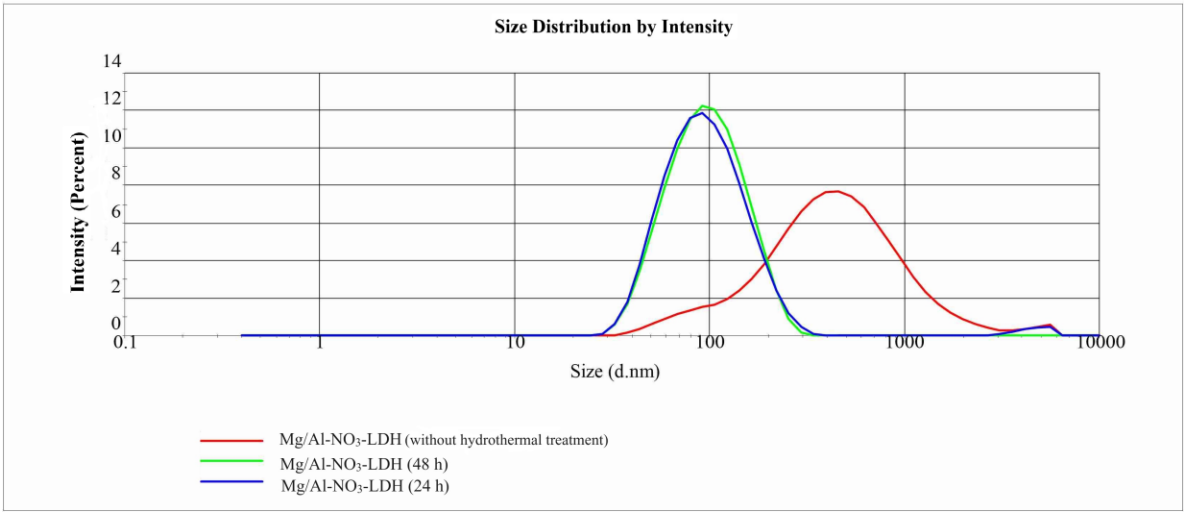

Figure 5. Effect of hydrothermal treatment time on the nMg/Al-NO_3-LDH particle size

3.3 Colloidal Stability of nMg/Al-NO_3-LDH

A colloidal stability of nMg/Al-NO_3-LDH was carried out to determine the change in particle size, PDI and zeta potential in the duration of use depending on the time and +4 °C storage condition (Table 4). Results were taken in triplicate. According to Table 4, the measurement results show that the Z average varied slightly between 86.87±0.320 and 109.6±2.3 nm. Moreover, PDI values are located between 0.132±0.018 and 0.276±0.018. Although the results of zeta potential were very close to the value obtained in the first synthesis of nMg/Al-NO_3-LDH, it changed slightly within 5 weeks. nMg/Al-NO_3-LDH remains stable for 5 weeks.

Table 4. Colloidal stability of nMg/Al-NO_3-LDH stored at +4 ±1˚C for 5 weeks.

Time (Week)	*Z-average (nm)*	*PDI*	*Zeta potential (mV) ±SD*
After preparation	86.87±0.32	0.132±0.018	44.4±8.74
1	97.29±8.22	0.173±0,017	47.6±8.58
2	93.71±1.44	0.173±0.011	49.7±6.93
3	95.39±2.50	0.205±0.038	46.3±8.77
4	107.55±2.80	0.228±0.019	41.8±7.82
5	109.6±2.30	0.276±0.018	47.3±7.94

4. CONCLUSION

As a result, the synthesis of nMg/Al-NO_3-LDH was optimized in this study. The effects of time, temperature, and stirring rate on the size and zeta potential of nMg/Al-NO_3-LDH were evaluated. The most suitable condition for synthesis was 80 ˚C, 48 h and 250 rpm, and nanoparticles with the particle size of 86.87 nm, a PDI of 0.132, and a zeta potential (mV) of 44.4±8.74 were obtained. The colloidal stability of nMg/Al-NO_3-LDH was then monitored for 5 weeks. The prepared nanoparticles maintained physical stability for up to 5 weeks under +4±1˚C storage conditions. Insights from this study revealed important data on tailoring nMg/Al-NO_3-LDH for specific biological applications, from controlled release systems to advanced catalytic materials. Future studies on drug loading and biodistribution will increase the prospective importance of nMg/Al-NO_3-LDH prepared under optimum conditions.

REFERENCES

[1] Kameliya J., Verma A., Dutta P., Arora C., Vyas S., Varma R.S. (2023). "Layered Double Hydroxide Materials: A Review on Their Preparation, Characterization, and Applications." Inorganics 11, 121

[2] Gama B., Selvasembian R., Giannakoudakis D.A., Triantafyllidis K.S., McKay G., Meili L. (2022). "Layered Double Hydroxides as Rising-Star Adsorbents for Water Purification: A Brief Discussion." Molecules 27. 10.3390/molecules27154900

[3] Constantino V.R.L., Figueiredo M.P., Magri V.R., Eulálio D., Cunha V.R.R., Alcântara A.C.S., Perotti G.F. (2023). "Biomaterials Based on Organic Polymers and Layered Double Hydroxides Nanocomposites: Drug Delivery and Tissue Engineering." Pharmaceutics 15. 10.3390/pharmaceutics15020413

[4] Choy J.-H., Jung J.-S., Oh J.-M., Park M., Jeong J., Kang Y.-K., Han O.-J. (2004). "Layered double hydroxide as an efficient drug reservoir for folate derivatives." Biomaterials 25, 3059-3064. https://doi.org/10.1016/j.biomaterials.2003.09.083

[5] Mohanambe L., Vasudevan S. (2005). "Anionic clays containing anti-inflammatory drug molecules: Comparison of molecular dynamics simulation and measurements." The Journal of Physical Chemistry B 109, 15651-15658

[6] Li L., Gu W., Chen J., Chen W., Xu Z.P. (2014). "Co-delivery of siRNAs and anti-cancer drugs using layered double hydroxide nanoparticles." Biomaterials 35, 3331-3339. https://doi.org/10.1016/j.biomaterials.2013.12.095

[7] Kura A.U., Ain N.M., Hussein M.Z., Fakurazi S., Hussein-Al-Ali S.H. (2014). "Toxicity and metabolism of layered double hydroxide intercalated with levodopa in a Parkinson's disease model." Int J Mol Sci 15, 5916-5927. 10.3390/ijms15045916

[8] Wong Y., Markham K., Xu Z.P., Chen M., Max Lu G.Q., Bartlett P.F., Cooper H.M. (2010). "Efficient delivery of siRNA to cortical neurons using layered double hydroxide nanoparticles." Biomaterials 31, 8770-8779. 10.1016/j.biomaterials.2010.07.077

[9] Chen C., Wang P., Lim T.-T., Liu L., Liu S., Xu R. (2013). "A facile synthesis of monodispersed hierarchical layered double hydroxide on silica spheres for efficient removal of pharmaceuticals from water." Journal of Materials Chemistry A 1, 3877-3880. 10.1039/C3TA10197E

[10] Janani F.Z., Taoufik N., Khiar H., Boumya W., Elhalil A., Sadiq M., Puga A.V., Barka N. (2021). "Nanostructured layered double hydroxides based photocatalysts: Insight on synthesis methods, application in water decontamination/splitting and antibacterial activity." Surfaces and Interfaces 25, 101263. https://doi.org/10.1016/j.surfin.2021.101263

[11] Özgümüş S., Gök M.K., Bal A., Güçlü G. (2013). "Study on novel exfoliated polyampholyte nanocomposite hydrogels based on acrylic monomers and Mg–Al–Cl layered double hydroxide: Synthesis and characterization." Chemical Engineering Journal 223, 277-286. https://doi.org/10.1016/j.cej.2013.02.098

[12] Mishra G., Dash B., Pandey S. (2018). "Layered double hydroxides: A brief review from fundamentals to application as evolving biomaterials." Applied Clay Science 153, 172-186. https://doi.org/10.1016/j.clay.2017.12.021

[13] Liu L., Deng Q., White P., Dong S., Cole I.S., Dong J., Chen X.-B. (2022). "Hydrothermally prepared layered double hydroxide coatings for corrosion protection of Mg alloys – a critical review." Corrosion Communications 8, 40-48. https://doi.org/10.1016/j.corcom.2022.07.001

[14] He C., Hu Y., Yin L., Tang C., Yin C. (2010). "Effects of particle size and surface charge on cellular uptake and biodistribution of polymeric nanoparticles." Biomaterials 31, 3657-3666. https://doi.org/10.1016/j.biomaterials.2010.01.065

[15] Ladewig K., Xu Z.P., Lu G.Q. (2009). "Layered double hydroxide nanoparticles in gene and drug delivery." Expert Opin Drug Deliv 6, 907-922. 10.1517/17425240903130585

[16] Costa F.R., Leuteritz A., Wagenknecht U., Jehnichen D., Häußler L., Heinrich G. (2008). "Intercalation of Mg–Al layered double hydroxide by anionic surfactants: Preparation and characterization." Applied Clay Science 38, 153-164. https://doi.org/10.1016/j.clay.2007.03.006

[17] Molano-Mendoza M., Donneys-Victoria D., Marriaga-Cabrales N., Angel Mueses M., Puma G.L., Machuca-Martínez F. (2019). "Dataset on infrared spectroscopy and X-ray diffraction patterns of Mg-Al layered double hydroxides by the electrocoagulation technique." Data Brief 27, 104564. 10.1016/j.dib.2019.104564

[18] Jin S., Ye K. (2007). "Nanoparticle-mediated drug delivery and gene therapy." Biotechnol Prog 23, 32-41. 10.1021/bp060348j

[19] Xu Z.P., Stevenson G., Lu C.-Q., Lu G.Q. (2006). "Dispersion and Size Control of Layered Double Hydroxide Nanoparticles in Aqueous Solutions." The Journal of Physical Chemistry B 110, 16923-16929. 10.1021/jp062281o

[20] Harrison R., Li L., Gu Z., Xu Z.P. (2017). "Controlling mesoporous silica-coating of layered double hydroxide nanoparticles for drug control release." Microporous and Mesoporous Materials 238, 97-104. https://doi.org/10.1016/j.micromeso.2016.04.031

[21] Zhang L.-x., Xie X.-x., Liu D.-q., Xu Z.P., Liu R.-t. (2018). "Efficient co-delivery of neo-epitopes using dispersion-stable layered double hydroxide nanoparticles for enhanced melanoma immunotherapy." Biomaterials 174, 54-66. https://doi.org/10.1016/j.biomaterials.2018.05.015

[22] Zuo H., Gu Z., Cooper H., Xu Z.P. (2015). "Crosslinking to enhance colloidal stability and redispersity of layered double hydroxide nanoparticles." J Colloid Interface Sci 459, 10-16. 10.1016/j.jcis.2015.07.063

[23] Dong H., Parekh H.S., Xu Z.P. (2015). "Particle size- and number-dependent delivery to cells by layered double hydroxide nanoparticles." Journal of Colloid and Interface Science 437, 10-16. https://doi.org/10.1016/j.jcis.2014.09.010

[24] Musumeci A.W., Mortimer G.M., Butler M.K., Xu Z.P., Minchin R.F., Martin D.J. (2010). "Fluorescent layered double hydroxide nanoparticles for biological studies." Applied Clay Science 48, 271-279. https://doi.org/10.1016/j.clay.2009.11.008

[25] Bilati U., Allémann E., Doelker E. (2005). "Development of a nanoprecipitation method intended for the entrapment of hydrophilic drugs into nanoparticles." European Journal of Pharmaceutical Sciences 24, 67-75. https://doi.org/10.1016/j.ejps.2004.09.011

[26] Choi G., Piao H., Kim M.H., Choy J.-H. (2016). "Enabling Nanohybrid Drug Discovery through the Soft Chemistry Telescope." Industrial & Engineering Chemistry Research 55, 11211-11224. 10.1021/acs.iecr.6b02971

[27] Dong H., Chen M., Rahman S., Parekh H.S., Cooper H.M., Xu Z.P. (2014). "Engineering small MgAl-layered double hydroxide nanoparticles for enhanced gene delivery." Applied Clay Science 100, 66-75. https://doi.org/10.1016/j.clay.2014.04.028

[28] Cao Z., Adnan N.N.M., Wang G., Rawal A., Shi B., Liu R., Liang K., Zhao L., Gooding J.J., Boyer C., Gu Z. (2018). "Enhanced colloidal stability and protein resistance of layered double hydroxide nanoparticles with phosphonic acid-terminated PEG coating for drug delivery." J Colloid Interface Sci 521, 242-251. 10.1016/j.jcis.2018.03.006

[29] Persano F., Batasheva S., Fakhrullina G., Gigli G., Leporatti S., Fakhrullin R. (2021). "Recent advances in the design of inorganic and nano-clay particles for the treatment of brain disorders." Journal of Materials Chemistry B 9, 2756-2784. 10.1039/D0TB02957B

[30] Danaei M., Dehghankhold M., Ataei S., Hasanzadeh Davarani F., Javanmard R., Dokhani A., Khorasani S., Mozafari M.R. (2018). "Impact of Particle Size and Polydispersity Index on the Clinical Applications of Lipidic Nanocarrier Systems." Pharmaceutics 10. 10.3390/pharmaceutics10020057

[31] Qin L., Wang W., You S., Dong J., Zhou Y., Wang J. (2014). "In vitro antioxidant activity and in vivo antifatigue effect of layered double hydroxide nanoparticles as delivery vehicles for folic acid." Int J Nanomedicine 9, 5701-5710. 10.2147/ijn.S74306

[32] Bhattacharjee S. (2016). "DLS and zeta potential – What they are and what they are not?" Journal of Controlled Release 235, 337-351. https://doi.org/10.1016/j.jconrel.2016.06.017

[33] Xu R. (2008). "Progress in nanoparticles characterization: Sizing and zeta potential measurement." Particuology 6, 112-115. https://doi.org/10.1016/j.partic.2007.12.002

[34] Xu Z.P., Jin Y., Liu S., Hao Z.P., Lu G.Q. (2008). "Surface charging of layered double hydroxides during dynamic interactions of anions at the interfaces." J Colloid Interface Sci 326, 522-529. 10.1016/j.jcis.2008.06.062

[35] Zhang Y., Evans J.R.G. (2012). "Alignment of layered double hydroxide platelets." Colloids and Surfaces A: Physicochemical and Engineering Aspects 408, 71-78. https://doi.org/10.1016/j.colsurfa.2012.05.033